

SUPPRESSION OF PREMIXED FLAMES BY WATER MIST IN MICROGRAVITY: FINDINGS FROM THE *MIST* EXPERIMENT ON STS-107

Angel Abbud-Madrid and J. Thomas McKinnon
Center for Commercial Applications of Combustion in Space
Colorado School of Mines, Golden, CO 80401
Ph: (303) 384-2300, E-mail: aabbudma@mines.edu, jmckinno@mines.edu

Francine K. Amon
National Institute of Standards and Technology (NIST)
Gaithersburg, MD 20899-8663
Ph: (301) 975-4913, E-mail: francine.amon@nist.gov

and

Suleyman Gokoglu
NASA Glenn Research Center
Cleveland, OH 44135
Ph: (216) 433-5499, E-mail: S.Gokoglu@grc.nasa.gov

ABSTRACT

A preliminary analysis of the results obtained from the Water-Mist Fire Suppression experiment (*Mist*) that flew on the STS-107 mission of the Space Shuttle is presented. The objective of *Mist* is to study the effects of droplet size distribution and water concentration on the burning velocity of a propagating premixed propane-air flame. Changes of the laminar flame speed and shape are used as the measure of flame suppression efficacy. Thirty-two tests were conducted with four different fuel-air equivalence ratios (0.6, 0.7, 1.0, and 1.3), two droplet size distributions (count median diameters of 20 and 30 μm), and water loadings (measured in water mass fraction) ranging from 0.0 to 0.1. The injection of water mist in microgravity resulted in a uniformly distributed and quiescent droplet cloud. Lean flames with a parabolic flame front monotonically slowed down to a steady-state velocity through the mist cloud. Small droplet size distributions are consistently more effective than larger ones in suppressing the propagation of lean flames with the effect of droplet size diminishing at the lowest burning velocities. Increased water loading always results in slower flames, with lean flames more easily suppressed than richer ones. Flame extinction was obtained for lean flames with water mass fractions under 0.05.

INTRODUCTION

The deficiency in replacing the chemical agents banned by the Montreal Protocols has led to an increasing interest in fine water mists as fire suppressants for several reasons, among them the lack of adverse environmental or health issues with water-based fire suppression systems and the promise of protecting water- and weight-sensitive areas due to the low requirements for total water flow. Water mist technology has been found effective for a wide range of applications

such as shipboard machinery, aircraft cabins, computers, and electronic equipment [1]. In addition, water mist may also find an application in spacecraft fire suppression systems. On a per unit-mass basis, water is as effective as Halon 1301, the agent currently used in the Space Shuttle, while water is more effective for surface and deep seated fires than carbon dioxide (CO_2), the agent selected for the International Space Station fire-extinguishing systems. Water is also non-toxic, non-corrosive, readily available in spacecraft for multiple uses, and deionized water may be used for fighting electrical fires. Moreover, agent cleanup operations may be achieved with dehumidifiers in the ventilation system. Consequently, the suppression properties of water mists are currently being investigated in the search for new fire suppression systems for the next generation of spacecraft.

Besides the obvious benefits of water mist for spacecraft applications, space also offers a unique environment for the study of fire suppression with water mists. To date, it is generally agreed that there is still no widely accepted interpretation of the interaction of a flame with a water mist, of the critical concentration of droplets and the optimum droplet size distribution required to suppress a flame, or of the fundamental mechanisms involved in flame extinguishment by a water mist. One of the main obstacles to obtaining such basic understanding is the difficulty of providing a simple, controlled experimental setup for the flame front/water mist interaction. Some of the difficulty stems from the problem of distributing and maintaining a homogeneous concentration of droplets throughout a chamber while gravity and water deposition loss on surfaces deplete the concentration and alter the droplet size by coalescence and agglomeration mechanisms. Experiments conducted in microgravity (μg) provide an ideal environment to study the fundamental interaction of water mists and flames by eliminating these distorting effects. In addition, μg eliminates the complex flow patterns induced between the flame front and the water droplets. The long duration and quality of μg in space flights provide the required conditions to perform the setup and monitoring of flame suppression experiments. In order to take advantage of this environment, the Water-Mist Fire Suppression experiment (*Mist*) was flown on the STS-107 mission of the Space Shuttle *Columbia* on January, 2003. It consisted of a series of microgravity tests that explored the effect of uniformly distributed clouds of polydisperse water mists on the speed and shape of propagating propane-air premixed flames. It is hoped that the results from these tests will provide important fundamental information that can be utilized in numerical models that will be used to design the next generation of fire suppressants not only for spacecraft, but for many applications on Earth as well.

EXPERIMENTAL APPARATUS AND APPROACH

A flow diagram and a three-dimensional model of the *Mist* flight apparatus with the main components of the experiment are shown in Fig. 1. In order to characterize the interaction of the water mist with the flame front, a mixture of propane (C_3H_8) and air is loaded in a transparent cylindrical tube of 6.3-cm diameter and 49.5-cm length. The C_3H_8 -air mixture was chosen for its ease of ignition, high flame luminosity, for its role as a base fuel to model the combustion of higher hydrocarbons, and for its wide use in many practical applications. In addition, two types of flame behavior are observed depending on mixture stoichiometry: continuous flames in lean mixtures and wrinkled flame fronts in rich mixtures. This behavior is caused by thermal-diffusive instabilities that depend on the Lewis number (Le) of the mixture [2].

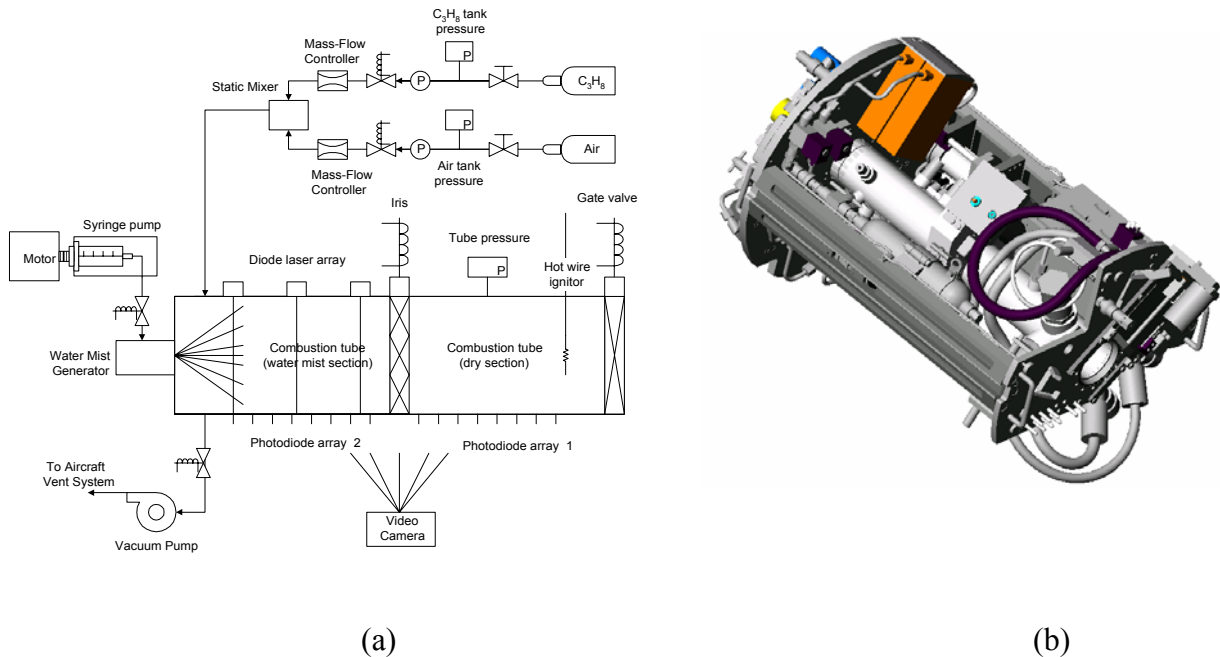


Figure 1. The *Mist* experiment: (a) Flow diagram of experimental apparatus and (b) Flight unit

The two gases are introduced in the tube from separate tanks through a static mixer using mass flow controllers. A polydisperse water mist generated by an ultrasonic atomizer is introduced in one half of the tube separated by an iris from the dry region. A light extinction system consisting of three diode lasers shining radially through the tube into three photodiode detectors is used to obtain droplet concentration (number density) data in different parts of the wet section. After the mist injection, the iris opens and the mixture is ignited in the dry section while keeping the valve at that end of the tube open for an isobaric combustion process. In order to measure the flame suppression ability of a given water-mist droplet size and water concentration, the propagation velocity of the premixed flame is measured by a video camera and by an array of 16 photodiodes installed along the tube. The *Mist* experiment was designed, fabricated, assembled, and tested at the Center for Commercial Applications of Combustion in Space (CCACS) at the Colorado School of Mines (CSM) and later tested and integrated to the Combustion Module-2 (CM-2) at the NASA Glenn Research Center. This module flew in the SPACEHAB Research Double Module, which was in turn located in the payload bay of the Space Shuttle *Columbia*.

The original test matrix consisted of 34 tests with three different fuel-air equivalence ratios, lean, stoichiometric, and rich ($\phi = 0.7, 1.0, \text{ and } 1.3$), three droplet size distributions (count median diameters, CMD, of 20, 30, and 40 μm), and three water loadings, measured in water mass fraction (mass of suspended water per mass of gas) of $\omega_w = 0.06, 0.12, \text{ and } 0.18$. Upon the on-orbit integration of the *Mist* experiment into the Combustion Module (CM-2), a leak in the flame tube was detected at the beginning of the first test point. Extensive troubleshooting on the ground and meticulous repair work by the crew in orbit successfully solved the problem, albeit with critical time lost in the process. As a result of this setback, it was feasible to access the apparatus only once to change the mist nozzle, reducing the number of droplet sizes from three to two. Nevertheless, due to an efficient coordination of the various ground teams, remote command and data communications, and crew resources, the final test matrix consisted of 32

tests with four different fuel-air equivalence ratios, very lean, lean, stoichiometric, and rich ($\phi = 0.6, 0.7, 1.0, \text{ and } 1.3$), two droplet size distributions (CMD = 20 and 30 μm), and a variety of water mass fractions ranging from 0.0 to 0.1. The re-arrangement of the test matrix was also due to the unexpected findings that were discovered during the mission which prompted a constant reevaluation of the test parameters used in the experiment. Since this evaluation required an immediate analysis of the results after each test, over 90% of the information gathered in orbit was downlinked to Earth in the form of sensor and video-image data prior to the accident of *Columbia* during its atmospheric reentry and the premature end of the STS-107 mission.

RESULTS AND DISCUSSION

The objective of *Mist* is to study the effects of droplet size distribution and water concentration on the burning velocity of a propagating premixed flame. Consequently, changes of the laminar flame speed and shape are used as the measure of flame suppression efficacy. Premixed flame fronts stretch due to hydrodynamic forces as they propagate through a tube, acquiring a larger burning surface area [3]. The burning velocity is a fundamental property of flames and is distinguished from the flame speed observed in the tube by normalization of the flame front surface area. The equation relating flame speed to burning velocity is given by:

$$S_{BV} = S_L \left(\frac{A_D}{A_{FF}} \right) \quad (1)$$

where S_{BV} is the burning velocity, S_L is the laminar flame speed, A_D is the area of a disk (the cross-sectional area of the flame tube), and A_{FF} is the surface area of the flame front. Most of the tests performed with very lean ($\phi = 0.6$) and lean ($\phi = 0.7$) C_3H_8 -air flames exhibit smooth hemispherical flame fronts. The flame fronts tend to become wrinkled and break into cells as the stoichiometry becomes richer for the $\phi = 1.0$ and $\phi = 1.3$ cases. This behavior is caused by the unequal rates of diffusion of thermal energy and mass, which is characteristic of a mixture with a Lewis Number lower than unity [2]. In the presence of water droplets, these instabilities are accentuated by the quenching action of the water mist. Multiple local extinctions on the wrinkled flame front by water droplets result in increased flame curvature and thus in a larger ratio of the reactant diffusion rate to the heat loss rate. As a result, the flame front breaks up into various cellular fronts that tend to propagate independently of each other. The highly curved cells acquire a higher temperature and higher resistance to extinction by water. It is interesting to note that wrinkled flame fronts were also observed in near-extinction flames with $Le > 1.0$ when exposed to large water concentrations.

For this preliminary analysis only the burning velocity of the very lean and lean flames will be examined, leaving the stoichiometric and rich flames for the next phase of the investigation when an algorithm for calculating the surface area of wrinkled flames is available. The surface area of the very lean and lean flames is approximated by the surface area of a paraboloid defined by the flame diameter and width:

$$A_{FF} = \frac{\pi h^4}{6a^2} \left(\frac{4a^2}{h^2} + 1 \right)^{3/2} - 1 \quad (2)$$

where the flame width, h , is the axial distance from the leading edge of the flame to the point where the flame achieves its largest diameter and a is half of the flame diameter. These dimensions are illustrated in Fig. 2. Some of the thicker flames (larger values of h) appear to be better fit by a hemisphere. The error in using a paraboloid shape compared to a hemisphere was found to be about 8% in the worst case. In this case, a and h were about the same magnitude.

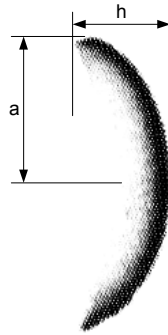


Figure 2. Flame front surface area approximation. The flame front is the darkened curve and propagates from left to right.

A mist behavior characterization study was performed that showed a consistent generation and suspension of an extremely uniform and quiescent cloud of droplets for several minutes as a result of the low microgravity levels (with negligible jitter or oscillations) experienced during free-drift periods in the Space Shuttle. Figure 3 shows how the mist was remarkably homogeneous after an initial transient period as it entered the tube. The initial recirculation patterns generated during the water mist injection disappear after a few seconds and the mist remains floating, almost motionless at the extremely low gravity levels encountered on the Space Shuttle ($\sim 10^{-6}g$). This uniformity in water concentration resulted in a uniform suppression of flames with a parabolic flame front monotonically slowing down to a steady-state speed through the mist cloud. An exception is the occurrence of intense distortion, pulsation, and break-up of flames near extinction at burning velocities close to 5 cm/s.

Figure 4 shows the burning velocities of the very lean and lean flames as a function of the position of the leading edge of the flame along the tube. Dry tests were conducted for all mixtures to establish a base burning velocity of a propagating flame with no water in the tube. Good agreement between experimental and literature values for burning velocity was observed for the lean flames, as shown in Fig. 4. Due to uncertainties in the dryness of the unburned gases inside the flame tube for the very lean case, literature values [4] of 13 cm/s and 23 cm/s for the burning velocities of the very lean and lean flames, respectively, will be used for comparisons in the following discussion. Figure 4 also shows the burning velocity of flames subjected to a fully saturated gas mixture and a uniform cloud of water mist with a water mass fraction of 0.002 (water loading of 0.2%) and a droplet size distribution of $CMD = 20 \mu m$. After a rapid initial decrease in burning velocity as the flame propagates through the wet section of the tube, it takes longer for the lean flame to reach a steady value as compared with the very-lean flame.

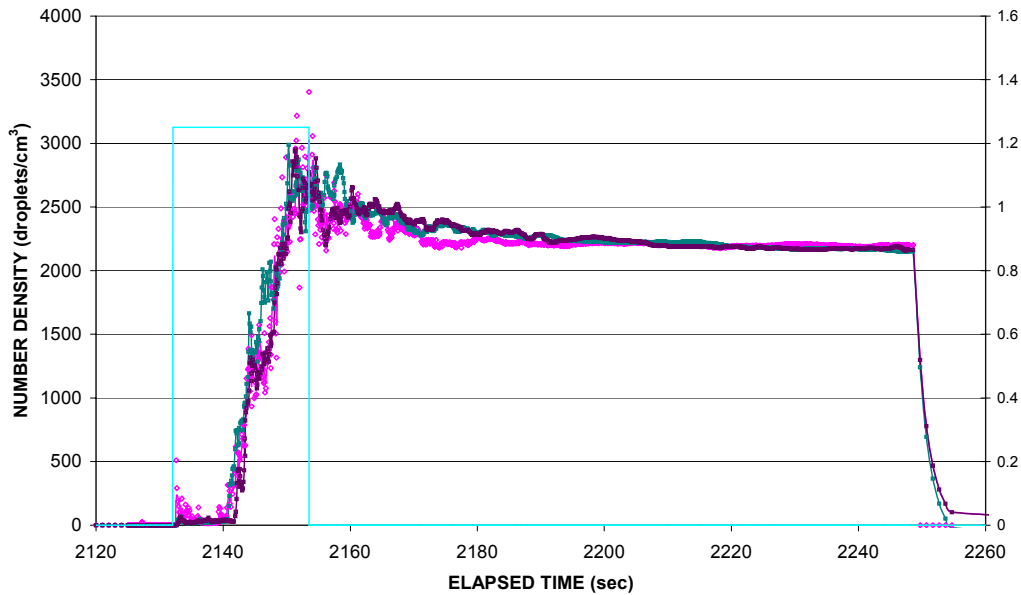


Figure 3. Water mist concentration (in number density) over time is measured by three detectors positioned along the misted section of the flame tube. Mist injection occurs during the initial rapid rise of the detectors signals (inside rectangle). For this test, the mist was allowed to become quiescent for about 90 s.

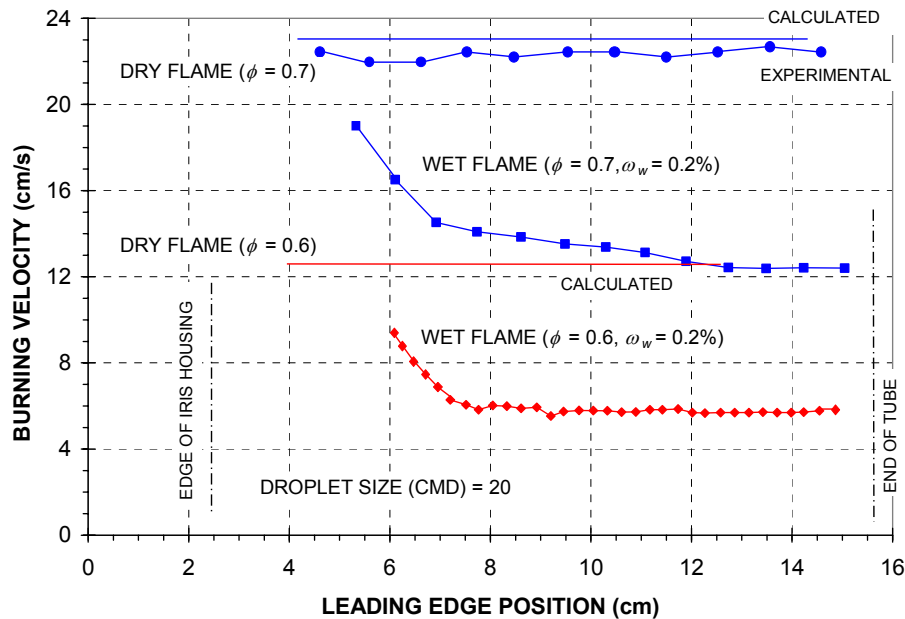


Figure 4. Flame burning velocities as a function of the position of the leading edge of the flame along the tube for dry and wet very-lean ($\phi = 0.6$) and lean ($\phi = 0.7$) propane-air flames with a water loading of 0.2% and a droplet size distribution of $CMD = 20 \mu\text{m}$.

The $\phi = 0.7$ flames start to stabilize at a leading edge position of about 13 cm, while the $\phi = 0.6$ flames have more consistent burning velocities that stabilize at a leading edge position of approximately 9 cm. The slower, weaker, less robust very-lean flames burn at a lower

temperature and are more easily suppressed, reaching their steady burning velocities faster than the stronger, more resilient lean flames; in the following discussions, comparisons of the burning velocities of suppressed flames are made using these steady values. Also shown in Fig. 4 is the effect of water on flames with different stoichiometry. Equal water concentrations have a larger effect on the leaner, weaker flames. A water loading of 0.2% with a mist droplet size of $CMD=20\ \mu\text{m}$ imparts a 46% decrease in the burning velocity of a C_3H_8 -air flame having $\phi = 0.7$ and a 55% decrease for a flame having $\phi = 0.6$.

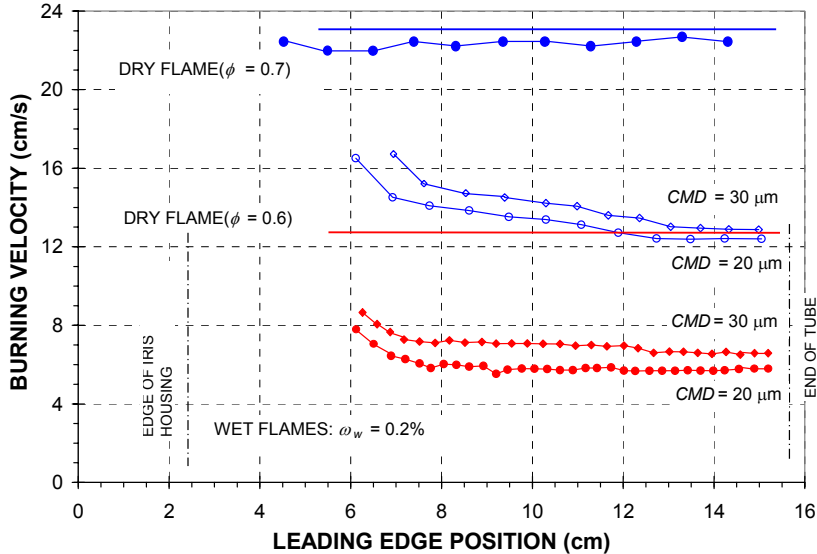


Figure 5. Effect of droplet size distribution on the burning velocity of very-lean ($\phi = 0.6$) and lean ($\phi = 0.7$) propane-air flames subjected to a water loading of 0.2%.

Figure 5 shows the effect of droplet size (CMD of 20 and 30 μm) on very-lean and lean flames subjected to a fully saturated gas mixture and a uniform cloud of water mist with a water loading of 0.2%. Droplet size distributions with smaller mean droplet diameters are more effective than larger droplets at slowing down flame propagation. For a water loading of 0.2% and a $\phi = 0.6$ flame, the burning velocity is reduced by 49% from its dry-flame value with a $CMD = 30\ \mu\text{m}$, whereas the burning velocity is reduced by 55% with droplets having a CMD of 20 μm . Similar behavior is shown for the $\phi = 0.7$ case. The larger effect on burning velocity reduction with weaker flames that was mentioned in the previous paragraph is again clearly seen here with the two droplet size distributions studied.

Figures 6 and 7 present the effect of water concentration on the burning velocity of lean flames ($\phi = 0.7$) subjected to a uniform cloud of water mist with droplet size distributions of $CMD = 30$ and 20 μm , respectively. At the larger droplet size of $CMD = 30\ \mu\text{m}$ and moist air^{*}, the burning velocity is reduced by 40% from the dry-flame value. For a 0.2% water loading (practically a saturated mixture) the burning velocity is reduced by 44%. When the water loading is increased to 2.5% the burning velocity is further reduced to about 76% of the dry-flame value.

^{*} Moist air refers to a water vapor concentration below 100% relative humidity at standard temperature and pressure. The droplets injected into the flame tube evaporated completely before the flame was ignited.

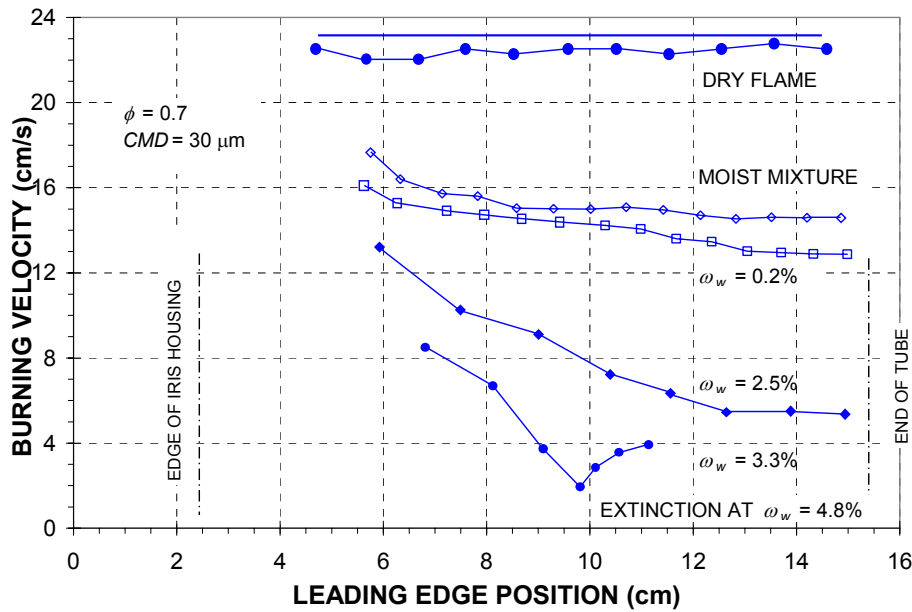


Figure 6. Effect of water concentration on the burning velocity of lean ($\phi = 0.7$) propane-air flames subjected to a droplet size distribution of $CMD = 30 \mu\text{m}$.

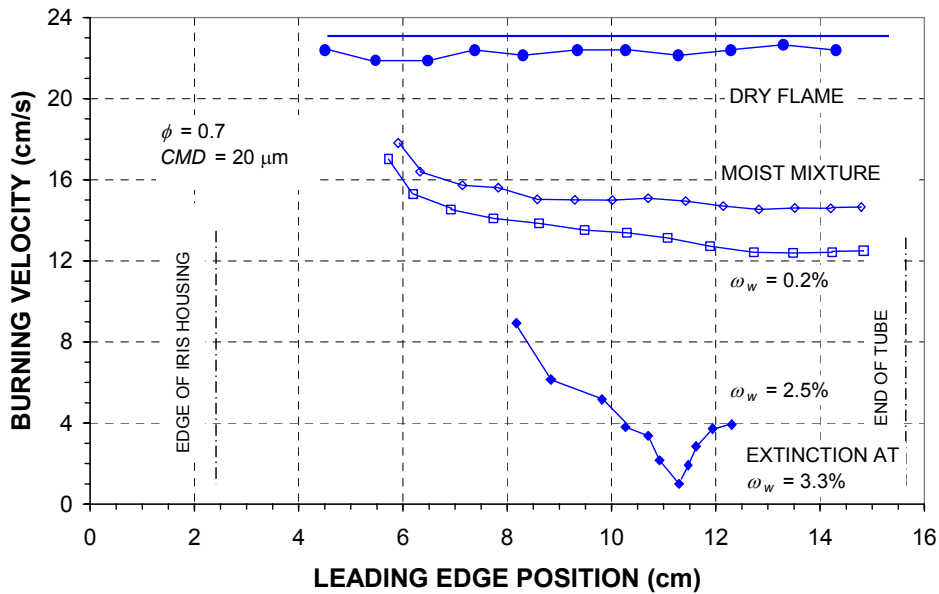


Figure 7. Effect of water concentration on the burning velocity of lean ($\phi = 0.7$) propane-air flames subjected to a droplet size distribution of $CMD = 20 \mu\text{m}$.

At a 3.3% water loading, the flame struggles to propagate along the flame tube. The “bouncing” appearance of the burning velocity is a result of the flame’s surface area expanding and contracting as the flame falters and recovers. This flame is practically on the verge of extinction. Finally, at a mist concentration of 4.8% the flame is rapidly extinguished as it enters the misted region of the flame tube. Similar behavior is observed in Fig. 7 with a $\phi = 0.7$ flame subjected to various water loadings with a droplet size distribution of $CMD = 20 \mu\text{m}$. For this smaller droplet size, the pulsating behavior observed near extinction occurs at a smaller water

loading of 2.5%, with a total extinguishment observed at 3.3%. It is interesting to note that small droplets consistently have a larger effect on the burning velocity than bigger droplets; larger concentrations of water are required to extinguish a flame with larger droplets.

Parallel to the experimental work, the effects of droplet diameter, number density, stoichiometry and the major water mist fire suppression mechanisms have been incorporated into a numerical model developed for premixed flames [5]. The computational model uses a hybrid Eulerian-Lagrangian formulation to simulate the two-phase, flame/mist interaction. Currently, the model is capable of simulating the free propagation of planar, premixed laminar flames of various stoichiometries and their interaction with monodisperse water droplets. Gas-phase chemical kinetics, thermodynamic, and transport properties are handled by the PREMIX software [6] and are used in the Eulerian representation of the propagating flame. Various chemical databases are used for the fuel-air reaction mechanisms. This formulation is then coupled with droplet source terms from Lagrangian equations of mass, momentum, energy, and particle flux fraction. The interaction between the two phases is modeled using an imaginary gas packet that follows the droplet. This algorithm facilitates a stable coupling between the phases, yet permits solving the gas-phase equations and droplet equations separately.

This numerical model simulates the conditions of the *Mist* experiment with two important exceptions. First, the model uses the GRI-Mech chemical reaction mechanism [7], which is appropriate for CH₄-air flames, but not for C₃H₈-air flames. Although no significant differences in the model results are expected when comparing the effects of suppression mechanisms on the two flame mixtures, work is ongoing to include a C₃H₈-air chemical reaction mechanism for a closer comparison with experimental results. Second, the model uses a monodisperse mist droplet size distribution. Monodisperse size distributions are much easier to handle than polydisperse size distributions in computational models, but rarely (if ever) occur in the natural world. Considering the differences between the numerical model as it currently exists and the *Mist* experiment, direct quantitative comparisons are not yet possible. It is, however, possible to compare trends in the CH₄-air modeling results with the experimental results. In Fig. 8, the effect of water loading on burning velocity is shown for CH₄-air flames for a range of droplet sizes (D_p) and for two stoichiometries ($\phi = 0.6$ and 0.7). The burning velocity becomes more sensitive to water loading as the droplets decrease in size from 50 μm to 15 μm . Interestingly, below 20 μm the droplet size ceases to have a significant impact on burning velocity in the $\phi = 0.7$ flames, while this effect occurs at a larger droplet size of 40 μm for the $\phi = 0.6$ flames. This is because very small droplets evaporate before reaching the flame reaction zone while larger droplets survive the reaction zone, passing through it without utilizing their full suppressive potential. Thus, water loading becomes more important as the burning velocity decreases.

The results of the *Mist* tests also indicate that the burning velocity is reduced with droplet size and water loading as predicted numerically. The suppression lines for the experimental C₃H₈-air flames on a plot comparable to Fig. 8 would be slightly steeper for the droplet size distributions tested than the ones shown in the graph. Furthermore, the results from *Mist* explore for the first time the water suppressed near-extinction region at very low burning velocities which are possible to observe only under non-buoyant conditions. At these very low velocities (and as shown in Fig. 8) a droplet-size independent region exists which is exclusively dominated by water loading. As predicted by numerical calculations, the experiments performed in microgravity show that small droplet size distributions are consistently more effective than larger

ones in suppressing the propagation of lean premixed flames. However, it was observed that the effect of droplet size diminishes as the burning velocities become smaller. The discovery of a droplet-size-independent region, exclusively dominated by water loading, is a result of the ability to suppress flames to extremely slow burning velocities in microgravity (around a few cm/s), which are impossible to obtain in normal gravity due to the distorting effect of buoyancy on weakly propagating flames. It is suspected that this behavior may be due to the long residence time of the droplets ahead of the flame that allows them to vaporize and heat up before reaching the flame front, thus exhibiting the same suppression effect regardless of their size.

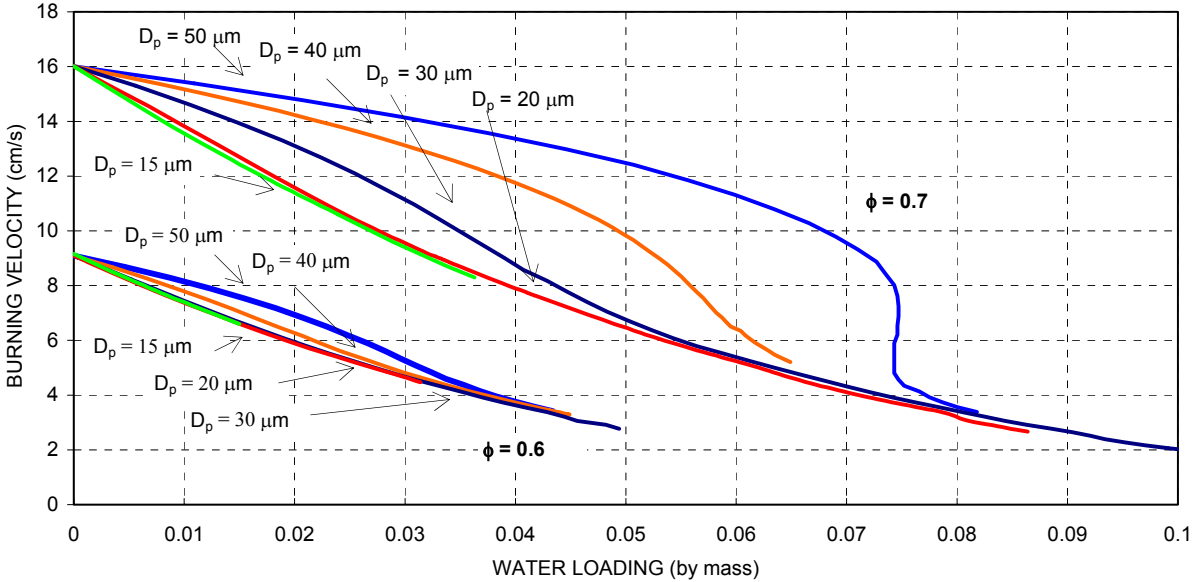


Figure 8. Numerical calculations of burning velocity as a function of water loading and droplet size (D_p) for CH_4 -air flames with an equivalence ratio of 0.6 and 0.7.

The model also predicts that lean flames are more vulnerable to suppression by mist, compared to stoichiometric flames, because they are relatively weaker due to an excess of oxygen. The *Mist* experimental results support this conclusion. The model also predicts that water mist is more effective at suppressing rich flames ($\phi > 1$) than lean flames. This result contradicts the experiments because the model does not take into account the effect of flame front curvature, which has a significant influence on the resilience of rich flames.

Several other groups have investigated water mist suppression of CH_4 -air flames, both numerically and experimentally. Lentati and Chelliah [8, 9] found that monodisperse droplets smaller than $20\ \mu\text{m}$ tended to follow the gas flow and evaporate in the most effective region of a counterflow diffusion flame. The optimum droplet size for their work was found to be $15\ \mu\text{m}$. Thomas [10] developed a numerical model for laminar premixed CH_4 -air flames which predicts an optimum monodisperse droplet diameter of $10\ \mu\text{m}$ and an optimum water loading density of 0.05 to $0.06\ \text{kg/m}^3$. A study of premixed C_3H_8 -air flame speeds in microgravity, using standard flammability limit tubes, was conducted by NASA in the late 1980s [11]. The unsuppressed laminar flame speeds reported for lean flames in microgravity show good agreement with the dry flame speeds in this work. It is difficult to compare the properties and suppression of premixed flames in microgravity with premixed flames in normal gravity because buoyancy driven flow

transports reactants away from the reaction zone in upwardly propagating flames and excessive heat is lost to the tube walls in downwardly propagating flames. Due to the absence of buoyant distortions, the present investigation provides results closer to fundamental values of flame suppression and extinction by water mist.

CONCLUSIONS

An investigation of the effect of water mists on premixed flame propagation was conducted on the STS-107 mission of the Space Shuttle *Columbia* to take advantage of the prolonged microgravity environment to study the effect of uniformly distributed clouds of polydisperse water mists on the speed and shape of propagating propane-air premixed flames. Thirty-two tests were conducted with four different fuel-air stoichiometries ($\phi = 0.6, 0.7, 1.0, \text{ and } 1.3$), two droplet size distributions (count median diameters of 20 and 30 μm), and a variety of water loadings (measured in water mass fraction) ranging from 0.0 to 0.1. All tests were conducted during free-drift periods and over 90% of the data gathered in orbit were downlinked to Earth in the form of sensor and video-image data.

The first data analysis has concentrated on the behavior of water mist injection, distribution, and suspension in microgravity, as well as on the effects of droplet size and water loading on very-lean and lean propane-air flames ($\phi = 0.6 \text{ and } 0.7$). Preliminary results indicate that the injection of water mist in microgravity resulted in a uniformly distributed and quiescent cloud of droplets. This uniform suspension of water droplets resulted in the controlled suppression of well-behaved flames with a parabolic flame front monotonically slowing down to a steady-state velocity through the mist cloud. An exception is the occurrence of intense distortion, pulsation, and break-up of flames near extinction at burning velocities close to 5 cm/s.

The preliminary results of the *Mist* experiment show good agreement with trends obtained by the numerical predictions of a computational model that uses a hybrid Eulerian-Lagrangian formulation to simulate the two-phase, flame/mist interaction. Small droplet size distributions are consistently more effective than larger ones in suppressing the propagation of lean premixed flames. However, it was observed that the effect of droplet size diminishes as the burning velocities become smaller. The discovery of a droplet-size-independent region, exclusively dominated by water loading, is a result of the ability to suppress flames to extremely slow burning velocities in microgravity (around a few cm/s), which are impossible to obtain in normal gravity due to the distorting effect of buoyancy on weakly propagating flames. It is suspected that this behavior may be due to the long residence time of the droplets ahead of the flame that allows them to vaporize and heat up before reaching the flame front, thus exhibiting the same suppression effect regardless of their size. Increased water loading always results in slower flames, with leaner, weaker flames ($\phi = 0.6$) more easily suppressed than richer ones ($\phi = 0.7$). Flame extinction was successfully obtained for both stoichiometries with water mass fractions under 0.05. Work is still ongoing in the numerical model to include a C_3H_8 -air chemical reaction mechanism and polydisperse sprays for a closer comparison with experimental results. Stoichiometric and rich flames, as well as other unusual flame behavior, such as flame front breakup and pulsating flames, are still under investigation.

In general, the effectiveness of water mist as a fire suppressant depends strongly on the ability of the mist droplets to penetrate to and evaporate in the flame reaction zone. The full effect of the

fire suppression mechanisms attributed to water mist is realized for any experimental environment or flame type where the droplets are as small as possible yet still large enough to reach the reaction zone. In microgravity the buoyant forces that would normally act to remove the smallest droplets in a polydisperse droplet size distribution are absent, therefore the full suppressive potential of the water mist is utilized. In addition, the extremely low burning velocities observed in microgravity increase the residence time of the droplets at the flame front, allowing a more complete vaporization of the water mist. Therefore, the fundamental values of optimum droplet size and concentration required to extinguish a flame in the presence of a water mist cloud are only obtained in μg conditions. It is hoped that the results from these tests will provide important fundamental information that can be utilized in numerical models that will be used to design the next generation of fire suppressants on spacecraft, as well as on Earth.

ACKNOWLEDGMENTS

This work is supported through the Center for Commercial Applications of Combustion in Space at the Colorado School of Mines under NASA Cooperative Agreement Number NCC8-238. We gratefully acknowledge the help of all CM-2 personnel at NASA GRC, of John West at NASA MSFC, of Edward Riedel, David Petrick, James Johnson, and Ed Ziemba during *Mist* mission operations at the NASA JSC Payload Control Center, of Abhijit Modak at CSM for the numerical calculations, and of the former CCACS director, Frank Schowengerdt. We also thank the financial and technical support of our industrial partners, FOGCO Systems, Inc. and MicroCool, Division of Nortec Industries, Inc. A special recognition and our most heartfelt appreciation go to the astronauts of the STS-107 mission of the Space Shuttle *Columbia* whose efforts and dedication during the operation of the *Mist* experiment guaranteed the success of the project.

REFERENCES

1. Mawhinney, J. R. and Solomon, R., "Water Mist Fire Suppression Systems," in *The Fire Protection Handbook*, 18th ed., edited by A.E. Cote, Boston, National Fire Protection Association, pp. 216-248, 1997.
2. Abbud-Madrid, A. and Ronney, P. D., "Effects of Radiative and Diffusive Transport Processes on Premixed Flames near Flammability Limits," *Proceedings of the Combustion Institute*, **23**, pp. 423-431, 1990.
3. Lewis, B. and von Elbe, G., *Combustion, Flames and Explosions of Gases*, 3rd ed., Orlando FL, Academic Press, 1987.
4. Gottgens, J., Mauss, F., and Peters, N., "Analytical Approximations of Burning Velocities and Flame Thicknesses of Lean Hydrogen, Methane, Ethylene, Ethane, Acetylene, and Propane Flames," *Proceedings of the Combustion Institute*, **24**, pp. 129-135, 1992.
5. Yang, W. and Kee, R. J., "The Effect of Monodispersed Water Mists on the Structure, Burning Velocity, and Extinction Behavior of Freely Propagating, Stoichiometric, Premixed, Methane-Air Flames," *Combustion and Flame*, **130**, pp. 322-335, 2002.

6. Kee, R. J., Grcar, J. F., Miller, A., and Meeks, E., "PREMIX: A Fortran Program for Modeling Steady Laminar One-Dimensional Premixed Flames," Sandia National Laboratories, 1998.
7. Bowman, C. T., et al., *GRI-Mech: An Optimized Detailed Chemical Reaction Mechanism for Methane Combustion and NO Formation and Reburning*, Gas Research Institute, 1997.
8. Lentati, A. M. and Chelliah, H. K., "Dynamics of Water Droplets in a Counterflow Field and their Effect on Flame Extinction," *Combustion and Flame*, **115**, pp. 158-179, 1998.
9. Lentati, A. M. and Chelliah, H. K., "Physical, Thermal and Chemical Effects of Fine-Water Droplets in Extinguishing Counterflow Diffusion Flames," *Proceedings of the Combustion Institute*, **27**, 1998.
10. Thomas, G. O., "The Quenching of Laminar Methane-Air Flames by Water Mists," *Combustion and Flame*, **130**, pp. 147-160, 2002.
11. Wherley, B.L. and Strehlow, R. A., "The Behavior of Fuel-Lean Premixed Flames in a Standard Flammability Limit Tube Under Controlled Gravity Conditions," Aeronautical and Astronautical Engineering Dept. Report, University of Illinois.